Available online at www.CivileJournal.org

Civil Engineering Journal

(E-ISSN: 2476-3055; ISSN: 2676-6957)

Vol. 11, No. 07, July, 2025

Prediction the Dynamic Modulus of Hot Asphalt Mix Using Genetic Algorithms and Neural Network Modeling

Shadi M. Hanandeh [1*], Frank I. Aneke [2], Zaid Alajlan [3], Shadi Al Khateeb [4], Ruba A. Alkharabsheh [1]

[1] *Department of Civil Engineering, Faculty of Engineering, Al-Balqa Applied University, Al-Salt, 19117, Jordan.*

[2] *Geotechnics and Materials Development Research Group (GMDRg) Civil Engineering, University of KwaZulu-Natal, Durban 4004, South Africa.*

[3] *Department of Civil and Construction Engineering, College of Engineering, Imam Abdulrahman Bin Faisal University, Dammam 31451, Saudi Arabia.*

[4] *Department of Materials Engineering, Faculty of Engineering, Al-Balqa Applied University, Al-Salt, 19117, Jordan.*

Received 22 April 2025; Revised 17 June 2025; Accepted 26 June 2025; Published 01 July 2025

Abstract

The dynamic modulus is a fundamental characteristic of asphalt concrete and expresses the stiffness properties of a hot mix asphalt mixture as a function of temperature and loading rate. This study used artificial neural network modeling and genetic algorithms to evaluate the asphalt concrete dynamic modulus. The experimental database was collected from LTPP DATA that used in the ANN and genetic algorithm development and modeling. The output for the two models was the asphalt concrete dynamic modulus. Moreover, mathematical models were employed to predict the dynamic modulus of asphalt concrete with different parameters. Following the establishment of the model designs, the deficiencies and strengths of the proposed models are evaluated using determination coefficient (R^2) values. The evaluation was performed by comparing the dynamic modulus of asphalt concrete predicted from four models with the dynamic modulus obtained from the experimental testing. Notably, the neural network models achieved precise calculations for models 1 and 2, with R^2 values of 0.96 and 0.93, respectively. The genetic algorithm models achieved R^2 values of 0.73 for model 1 and 0.64 for model 2. The two models, the genetic algorithm model and the artificial neural network model, contributed to the generation of two new empirical equations.

Keywords: Dynamic Modulus; Genetic Algorithms; Neural Network; Asphalt Concrete; Prediction.

1. Introduction

The dynamic modulus, or $|E*|$, is a function of temperature, loading rate, and material parameters that can be used to characterize the stress-strain relationship for asphalt mixtures under sinusoidal loading. One of the most important parameters used to assess rutting and fatigue cracking distress predictions in the Mechanistic-Empirical Pavement Design Guide (MEPDG) [1, 2] is the dynamic modulus, which is also one of the main design inputs in Pavement Mechanistic-Empirical (M-E) Design to characterize the basic linear viscoelastic material properties. Much work has been done to predict $|E*|$ from hot mix asphalt (HMA) material parameters, even though $|E*|$ plays a key role in pavement design and the related test process is time-consuming and expensive [3, 4]. In the design of flexible pavements, the dynamic modulus is a crucial parameter. According to Harran & Shalaby's 2009 report, "the dynamic modulus (|E*|) is the ratio of stress to strain under vibratory conditions, calculated from data obtained from either free or forced vibration

* Corresponding author: hanandeh@bau.edu.jo

http://dx.doi.org/10.28991/CEJ-2025-011-07-08

tests in shear, compression, or elongation". Predictive modeling is the practice of estimating outcomes from several predictor variables utilizing data mining techniques and probability theory. An initial model can be created using either a basic linear equation or a more sophisticated structure generated by a complex optimization technique [5].

There are various well-known predictive models for dynamic modulus; some are regression models, while others involve Artificial Neural Networks (ANN) and genetic programming [6]. Andrei et al. [7] employed 205 mixes and 2750 data points to improve the original Witczak model, which has since been reformed to use binder shear modulus rather than binder viscosity [8]. Christensen et al. [9] proposed a new predictive model for $|E*|$ that utilizes the law of mixtures. The data base for training the model included 206 $|E*|$ measurements from 18 different HMA combinations. Jamrah et al. [10] aimed to enhance predictive models for HMA in Michigan. They found a considerable divergence between measured and calculated $|E*|$ values, particularly at high temperatures and low frequencies. Al-khateeb et al. [11] created a novel predictive model based on the law of mixtures that may be employed across a wider range of temperature and loading frequencies, including higher temperatures and lower frequencies. The predictor variables in the model were voids in mineral aggregate and binder shear modulus.

Sakhaeifar et al. [12] created separate temperature-based models to estimate dynamic modulus throughout a large temperature range. The predictor variables utilized in the model included aggregate gradation, VMA, Voids Filled with Asphalt, air void, effective binder content, and bind er phase angel. Sakhaeifar et al. [12] suggested a modeling approach for estimating the dynamic modulus ($|E*|$) of asphalt mixtures using artificial neural networks (ANN). The accuracy of the ANN's predictions is greatly influenced by its design. The optimal architecture and effective variables were found using the Grey Wolf Optimizer (GWO). A huge dataset was used to create predictive models, including aggregate gradation, volumetric parameters, binder properties, test circumstances, and reclaimed asphalt pavement content. The results suggest that a hybrid ANN and GWO can provide a framework for estimating $|E*|$ with a Pearson correlation coefficient over 0.98. For pavement engineers, an intuitive graphical user interface was also created.

Zhang et al. [13] developed a dynamic modulus predictive model using smart rock sensing data in pavement engineering. The MMLS3 test used the ensemble artificial neural network (ANN) model to predict the dynamic modulus of asphalt mixtures. The results showed the model's feasibility and robustness, affirming its reliable stability. Future studies should expand the database to include an extensive range of materials and loading conditions for model verification. Huang et al. [14] used an artificial neural network (ANN) method with ensemble and weight optimization techniques to guess what the asphalt concrete's dynamic modulus (E*) would be. This study employed the random forest technique for input selection, examining various techniques such as evolutionary, backward, forward, and brute force, all of which were hybridized with random forest. The evolutionary random forest strategy was the best at choosing inputs. The most important variables to think about when making ANN models were binder G* (dynamic shear modulus), binder (phase angle), ρ 200, and V_{beff}. The researchers found that the artificial neural network-particle swarm optimization (ANNPSO) model outperformed the other models.

Another thing they discovered was that weight optimization strategies worked better than ensemble techniques at improving ANN's ability to predict the dynamic modulus of asphalt concrete. Genetic method trained BP neural network model with 263 parametric analysis data sets to predict projectile residual velocity and attitude angle under different penetration conditions. The GA BP neural network model in this research accurately predicts projectile penetration in reinforced concrete multilayer target plates' residual velocity and deflection angle. This model and the reserved 13 test sets yield irrelevant data. BPNN excels in learning non-linear connections through continuously iterations. The process of training includes estimating the error between output and expected data, then retroactively adjusting weights and thresholds to reduce the error. Local convergence, parameter modification, etc. are limitations of these methods. This makes most optimization difficulties difficult. Many of these methods support unconstrained optimization. When iterating, constrained optimization algorithms use different constraint handling methodologies to find the best solution. Because heuristic algorithms were flawed, improved algorithms for solution quality and computation efficiency were needed. The authors of the study was interested in combining local search algorithms with additional heuristics to make them more resilient [15, 16].

Zhang et al. [17] published a different study that used a new optimization method to find the Cohesive Zone Model (CZM) parameters that affect how asphalt mixtures break. The Kriging model was utilized as a stand-in model for the semicircular bending test conducted at intermediate temperatures. To improve computing performance, a pre-select operation was suggested. The approach demonstrated its ability to correctly quantify fracture mechanics in asphalt mixes, as evidenced by the simulations' agreement with experimental observations. Huang et al. [18] looked at the modulus properties of different high-modulus asphalt mixtures (HMAMs) and how they related to how well they prevented rutting. The results indicated that the dynamic modulus of HMAMs fluctuates in response to changes in both loading frequency and testing temperature. The correlation between the ratio of dynamic modulus at low frequency to high frequency and dynamic stability in high-temperature situations is strong. For evaluating the resistance of HMAM to rutting, it is recommended to use two indicators: the absolute modulus and the ratio of the dynamic modulus at 0.1 Hz to the dynamic modulus at 25 Hz at a temperature of 55 °C. The study validates the practicality of utilizing these

assessment indices for evaluating various categories of HMAMs. Behnood & Golafshani [19] utilized biogeography-based programming (BBP) to develop predictive models for asphalt pavement behavior under various traffic and climate conditions. They developed two models using 4022 asphalt mixture samples and 90 asphalt mixture records. Both models provided excellent accuracy and outperformed the Witczak, Hirsch, and ANN models. The most influential factors were temperature and frequency.

Acharjee et al. [20] established two ANN-based prediction models for Colombian hot-mix asphalt mixtures. The models W-ANN and H-ANN outperformed earlier models in terms of dynamic modulus prediction. The models were trained, validated, and tested on 972 data points. Both models are sensitive to binder and mixture qualities, making them more practical for practitioners to utilize. These models can be utilized in Colombia for pavement design packages, reducing future testing requirements. Wang et al. [21] employed a combined technique to forecast dynamic modulus design parameters from Falling Weight Deflectometer (FWD) back-calculated modulus data. It creates dynamic modulus prediction models for in-service asphalt pavements utilizing fundamental model deduction and gene expression programming (GEP). The model improves design precision, refines residual life estimates, and identifies problematic segments, all of which are critical for the maintenance or reconstruction of existing pavements.

Also, Uwanuakwa et al. [22] described a new AHA-boosted model for estimating the dynamic modulus of hot mix asphalt concrete. Using data from NCHRP Report-547, the model outperformed known models. Incorporating test temperature, frequency, and asphalt content increased the model's accuracy by 1.23%. The study also identified the binder complex modulus as a significant predictor. However, a modest drop in R2 recommends additional validation. Hu et al. [23] presented an AI-powered IDEAL-E* test for asphalt mixtures, which addresses the high cost and complexity of previous methods. This novel approach streamlines the collection of E* data, allowing it to be used in AASHTO Pavement ME design software and harmonizes with current procedures in DOT and contractor quality control labs. Zeiada et al. [24] studied the dynamic modulus (|E*|) of hot-mix asphalt (HMA) and compares it to well-known regression models. Eight cutting-edge machine learning and deep learning methods are used: multiple linear regression, decision trees, support vector regression, ensemble trees, Gaussian process regression, artificial neural networks, recurrent neural networks, and convolutional neural networks. A database of 50 AC mixes is created, totaling 3,720 measurements. The bagging ETs, Gaussian process regression (GPR) with exponential kernel, and decision trees (DT) have the highest prediction accuracy, while bagging ETs have the simplest training and testing requirements.

2. Research Methodology

Figure 1 presents a structured workflow for predicting the dynamic modulus (|E*|) of hot mix asphalt using data-driven modeling techniques. The process starts with a comprehensive dataset from the LTPP database, which includes 7,400 dynamic modulus values from 346 asphalt mixtures. Preprocessing steps are then taken to ensure the input parameters are ready for analysis. Two primary modeling approaches are developed in parallel: Artificial Neural Networks (ANN) and Genetic Algorithms (GA). ANN models are implemented using MATLAB, while GA models are constructed using GeneXpro5.0. Both models are trained and tested using data subsets, and their predictive performances are evaluated using key metrics.

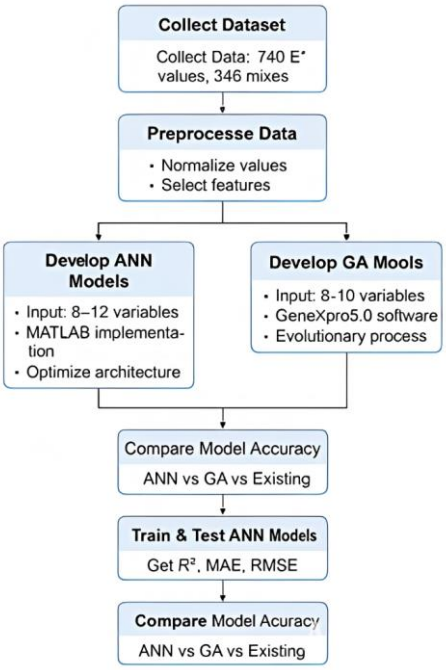

Figure 1. Flowchart for predicting the dynamic modulus (|E*|) of hot mix asphalt using Genetic Algorithms and Neural Network Modeling

A comparative analysis is conducted to determine the most accurate and reliable approach. Results show that ANN models significantly outperform other models, especially under extreme temperature and frequency conditions, making them the preferred method for predicting |E*|. The dataset underwent normalization using min-max scaling to ensure uniform input ranges across features. Outliers beyond three standard deviations were inspected and removed if deemed erroneous. Missing values were not present due to the comprehensive nature of the LTPP database. These preprocessing steps helped stabilize the model training process and improve convergence. The dataset was split into training (70%), validation (15%), and testing (15%) subsets to assess model performance. However, no external datasets or k-fold cross-validation were used. Future work should include testing on independent datasets or applying cross-validation to ensure model generalizability beyond the current data.

2.1. Experimental Program

In the experimental phase of this work, a cylindrical asphalt specimen undergoes testing in a chamber, where an axial force is applied at varying frequencies to determine its dynamic modulus. An environmental chamber controls the desired test specimen temperature, and the stress levels applied to the specimen are temperature-dependent. Table 1 below shows the recommended stress ranges for testing specimens at different temperatures.

Table 1. The stress ranges vs. temperature

Temperature °C (°F)	Range Stress range e (kPa)	Range Stress range e (psi)
-10 (14)	1400 to 2800	200 to 400
4 (40)	700 to 1400	100 to 200
21 (70)	350 to 700	50 to 100
37 (100)	140 to 250	20 to 50
54 (130)	35 to 70	5 to 10

To condition the test specimen, a sinusoidal stress is applied at 25 Hz for 200 cycles once the stress level is determined. Subsequently, the stress is applied at frequencies of 25 Hz, 10 Hz, 5 Hz, 1 Hz, 0.5 Hz, and 0.1 Hz, each for 200 cycles. Once the specimen completes all cycles at a given frequency, it should rest for two minutes before proceeding to the next frequency. Following the temperatures specified in Table 1, the specimen is then tested at a different ambient temperature.

The testing procedure begins with the lowest temperature and progresses sequentially to the highest temperature. After increasing the chamber testing temperature, the operator typically allows a waiting period of up to 6 hours to ensure the chamber and the specimens equilibrate at the new temperature before performing the subsequent test. To obtain average values for an asphalt sample, multiple specimens are evaluated at each temperature. Recording equipment, i.e., a load cell and three LVDTs directly mounted to the specimen, is used to measure the stress, recoverable strain, and permanent strain for each test. These parameters facilitate the calculation of the asphalt's phase angle and dynamic modulus. A standard asphalt specimen, measuring 6 in. 150 mm in height and 4 in. 100 mm in diameter, undergoes scoring using a scoring machine with a cooling system and a diamond bit, as presented in Figure 2. A SuperPave gyratory compactor is commonly employed for specimen creation and compaction. Additionally, a grinder and saw were utilized to trim the specimen to a size that guarantees level, smooth, and parallel edges. The impact of different combinations of particle sizes, void ratios, binder types, and other properties on specimen preparation and their subsequent influence on the asphalt mixture's dynamic modulus is investigated.

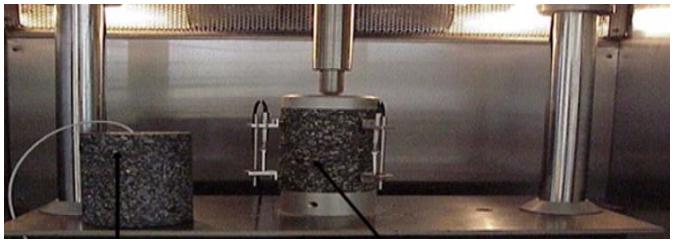

Figure 2. Instrumental setup and sample testing

It is known that the experimental measurements of the hot mix asphalt mixture's dynamic modulus are time-consuming, expensive, and require expert personnel. The study's goals are to figure out how to predict the dynamic modulus using genetic algorithms and artificial neural network models, as well as to create analytical models that can figure out how to predict the dynamic modulus (E*) of an asphaltic layer. Numerous studies on the available E* models have led to the conclusion that the properties of HMA and binders influence their prediction accuracy.

We will develop the predictive models in this work using artificial neural networks (ANN) and gene expression techniques. These models will be compared to previous studies to evaluate their performance. This study also aims to establish a correlation between the given set of volumetric and mechanical properties and the corresponding dynamic modulus values. This analysis would help optimize the dynamic modulus of asphalt mixes, thereby enhancing their

resistance to rutting and fatigue cracking in road construction across the USA. The variables in the study are temperature (T), loading frequency (f_c), phase degree (ε_b), grade of mix, asphalt content (AC), mix air void content (V_a%), effective binder content of the mix (V_{beff}%), and viscosity (h).

In this study, two methodologies were employed: ANN to model complex interactions between input and output variables and a genetic algorithm (GA) to establish the relationship between the inputs and output factors. ANN, a typical computational network modeling, incorporates hidden input and output layers, while GA, relying on Darwin's evolution theory, is considered the most efficient method for time and effort savings.

The gradation of the aggregates used in this study is presented in Figure 3. The distribution of particle sizes, indicated by cumulative retained percentages on standard sieves (No. 3/4, No. 3/8, No. 4, and No. 200), was used to analyze the aggregate structure of the hot mix asphalt. These gradation parameters are crucial because they directly affect the volumetric properties and ultimately the dynamic modulus (E*) of the asphalt mixture.

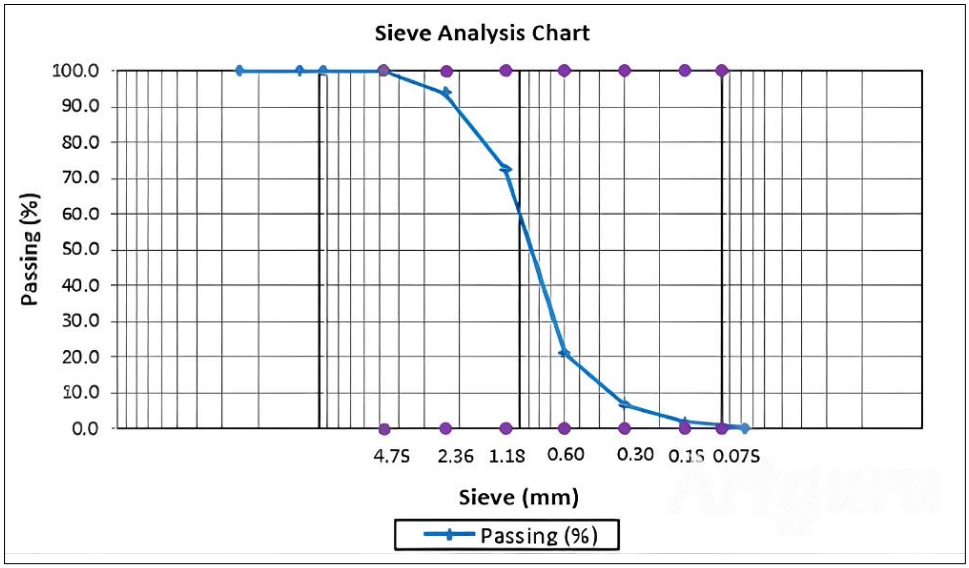

Figure 3. Aggregate gradation curve

2.2. Study Area

This study developed and trained new models to overcome the limitations of the Witczak model. Furthermore, this study employed a database containing 7400 |E*| values from 346 HMA combinations for this purpose. We replaced the bindings' viscosity and loading frequency (f) in the original Witczak model with the bindings' shear modulus (Gb*) and phase angle (b), respectively. The determination coefficient (R^2) between the measured and projected |E*| values of the new model improved to 0.96 for the first model and 0.93 for the second. This improvement indicates enhanced predictive accuracy. This study's primary objective was to establish a connection between the output (E*) and the various input factors (T, fc, |G*|, db, 34, etc.), as illustrated in Equation 2. Table 2 summarizes the standard mathematical parameters.

Table 2. Standard mathematical parameters for data that are utilized in model development

Parameter Name	Data Numbers	Max. value	Min. value	Mean. value
T	7400	130	0	70.52
f_c	7400	25	0.1	6.94
|G*|	7400	7386.6	0.02	995.97
δ_b	7400	90	11.86	58.98
ρ_{34}	7400	29.3	0	4.40
ρ_{38}	7400	56	0	24.98
ρ_4	7400	74	3	48.18
ρ_{200}	7400	11.8	0.4	4.96
AC	7400	10.2	3	5.53
Va	7400	18.1	0.1	6.73
V_{beff}	7400	25.1	6.08	10.76
h	7400	1.15833E+16	184297.0317	8.88851E+13
VMA	7400	34.64	10.33	17.5
E*	7400	8644878.528	10497.207	1311989.38

where: Temperature (T), Loading Frequency (f_c), Phase degree (ε_b), Gradation of Mix, Asphalt Content (AC), Mix Air Void Content (V_a%), Effective Binder Content of the Mix (V_{beff}%), Viscosity (h), void in mineral aggregate (VMA), asphalt concrete (AC), cumulative retained weight on the No. 4 sieve (ρ_4), cumulative retained weight on the No. 3/4-in. sieve (ρ_{34}), cumulative retained weight on the No. 3/8-in. sieve (ρ_{38}), and amount passing a No. 200 sieve (ρ_{200}).

2.3. Artificial Neural Network

An ANN is a widely employed computational modeling network that consists of hidden input and output layers. Its function is to simulate complex interactions between inputs and outputs or to obtain patterns within data. ANNs showcase the interconnection of the system through numeric weighting, adjusted according to inputs, experience, outputs, and processing. Simple interconnected adaptive processing components, often referred to as nodes or artificial neurons, comprise these networks, performing computations for knowledge representation and data processing [24–27].

The architecture of an ANN model includes nodes distributed across hidden layers, an input layer, and an output layer. The number of hidden layers can equal or exceed the number of inputs. The squared regression value influenced the decision to obtain the best performance in one hidden layer in both models through multiple trial and error processes. The study's database was compiled from prior research considering parameters leading to the "E*" outcomes.

This study employed an artificial neural network and genetic algorithm to predict the dynamic modulus of hot mix asphalt. ANN is a powerful model that correlates system components using numerical load based on input, processing, output, and experience. Maintaining ANN at an acceptable level and for prospects requires combining it with engineering methodologies. ANNs learn via experience, examples, and practice, like humans. Genetic algorithms are survival-of-the-fittest theoretical algorithms that use historical data. This improves search performance. This method excels in maintenance management, even with complex and changeable situations. The prediction of dynamic modulus (|E*|) was accomplished through the application of artificial neural networks (ANNs). The dynamic modulus serves as a crucial parameter in asphalt mixtures, acting as a primary input in EMPDG to predict rutting and fatigue cracking. Various factors, including air voids, asphalt content, temperature, and nominal maximum aggregate size, among others, contribute to its determination. This investigation employed two models: one with a single output and twelve inputs, and another with one output and eight inputs, respectively. These models were implemented using ANN to generate the expected outputs, which were then compared with the experimental outputs. This comparison was performed using specific inputs in each model. The database for this study was gathered from previous studies that took into account parameters leading to the determination of "E*" output. The ANN analysis was carried out using the MATLAB computer application.

2.4. Genetic Algorithm

A genetic algorithm represents an optimization approach that applies principles derived from Darwin's genetic determination theory to solve a problem. The central focus of the GA is to find the optimum value for a given function, aligning with Darwin's theory of evolution. The genetic algorithm involves three fundamental operations: selection, crossover, and mutations [28].

Using evolutionary tools like choice and variation, genetic algorithms explore functions that will appropriately fit data gathering. Friedberg pioneered the genetic algorithms field by developing a performance-oriented training algorithm. Cramer NL first introduced genetic programming, and Koza JR later improved it, leading to the development of sophisticated models. This study employed GeneXpro5.0, a gene expression programming model, to predict the dynamic modulus.

GeneXpro5.0 is a sophisticated data processing tool that solves diverse challenges and generates various models using vast volumes of heterogeneous data. It operates by locating codes in complex programming languages such as Visual Basic and Java, particularly in this study. Alongside compiling a comprehensive report on the process, several predictions are required to achieve optimal results. The authors have all reported the same approach with great efficiency in their predicted results [24, 29–32].

3. Results and Discussion

The performance of both ANN and GA models is described not only with R^2 values but also with error metrics such as MAE and RMSE. The influence of each variable (e.g., G*, AC, VMA) on dynamic modulus is discussed, providing engineering insights into the model results. Artificial Neural Networks (ANN) and Genetic Algorithms (GA) were selected due to their proven effectiveness in capturing complex, nonlinear relationships inherent in pavement material behavior. While other techniques such as Support Vector Machines (SVM), Decision Trees, and Ensemble Methods have demonstrated success in similar applications, ANN offers superior generalization for regression tasks with high-dimensional data, and GA provides flexibility in model structure development. These methods were also chosen based on their widespread availability in software tools like MATLAB and GeneXpro5.0, facilitating practical implementation and reproducibility.

3.1. Artificial Neural Network Models

The MATLAB software tool was used to extract the "E*" from the database, which was compiled from prior experiments incorporating relevant factors into account. The dynamic modulus is indicated by a single neuron for the output parameter. The main challenge lies in developing a suitable model capable of predicting an accurate E* value.

Consequently, modifying the number of hidden layers, the number of nodes for each hidden layer, and the number of epochs is necessary to obtain effective modeling control. The study employing ANN was executed using the MATLAB software application [33-37].

Figure 4 illustrates the structure of the neural model, displaying the twelve input parameters previously mentioned on the left side. This figure illustrates the layout of ANN Model 1, which includes twelve input parameters, one hidden layer with 13 neurons, and a single output neuron corresponding to the dynamic modulus (E*). This model configuration was selected after numerous iterations, yielding an R^2 value of 0.96 during training, indicating high accuracy. This visual representation aims to determine the optimal model by adjusting the number of hidden layers. Afterwards, we discovered that 13 neurons represent the optimal number of hidden layers, with each neuron on the right-hand side symbolizing the output, represented as E*. The neural network model provides accurate estimations of target values. Furthermore, the neural network model yields R^2 values of 0.96 and 0.95 for training and testing, respectively, offering acceptable estimation, as represented in Figure 5.

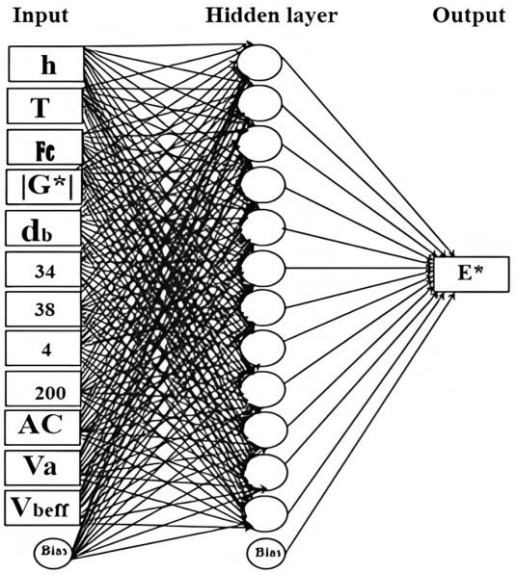

Figure 4. Input parameters, hidden layers, output, and biases for model 1 are represented by the structure of an ANN

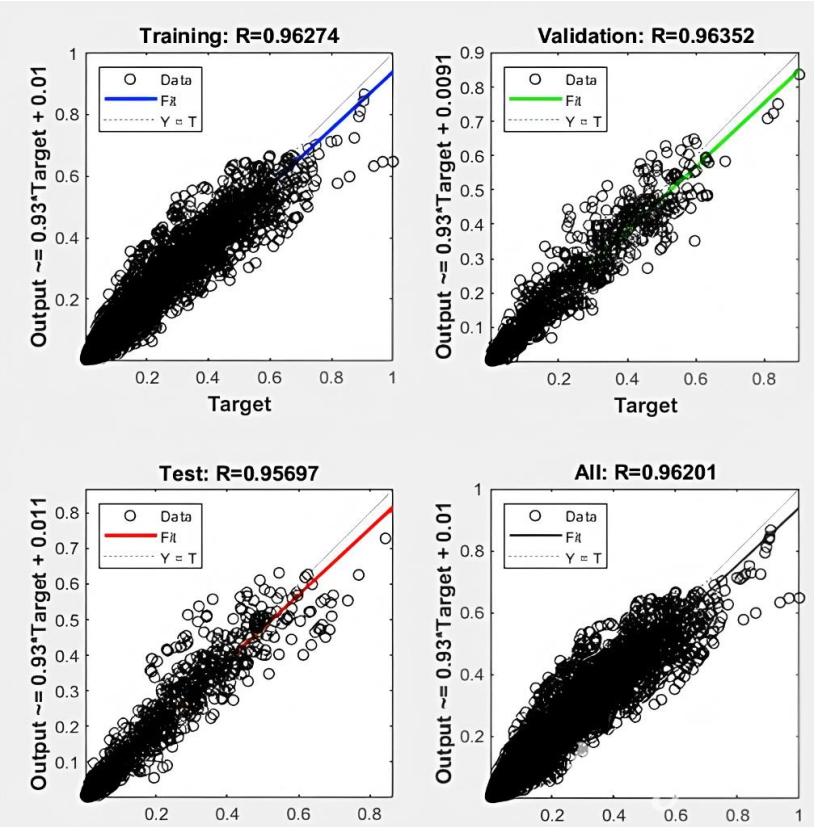

Figure 5. Model 1 training and testing data regression scheme of projected dynamic modulus against experimental dynamic modulus

The regression plot demonstrates a strong correlation between predicted and experimental values of E*. The closeness of the points to the regression line, with $R^2 = 0.96$, validates the model's ability to generalize well over the dataset. Figure 6 demonstrates the strong correlation between the observed E* and the measured E*. This figure confirms that both models maintain a strong linear relationship between experimental and predicted values, highlighting the robustness of the ANN approach.

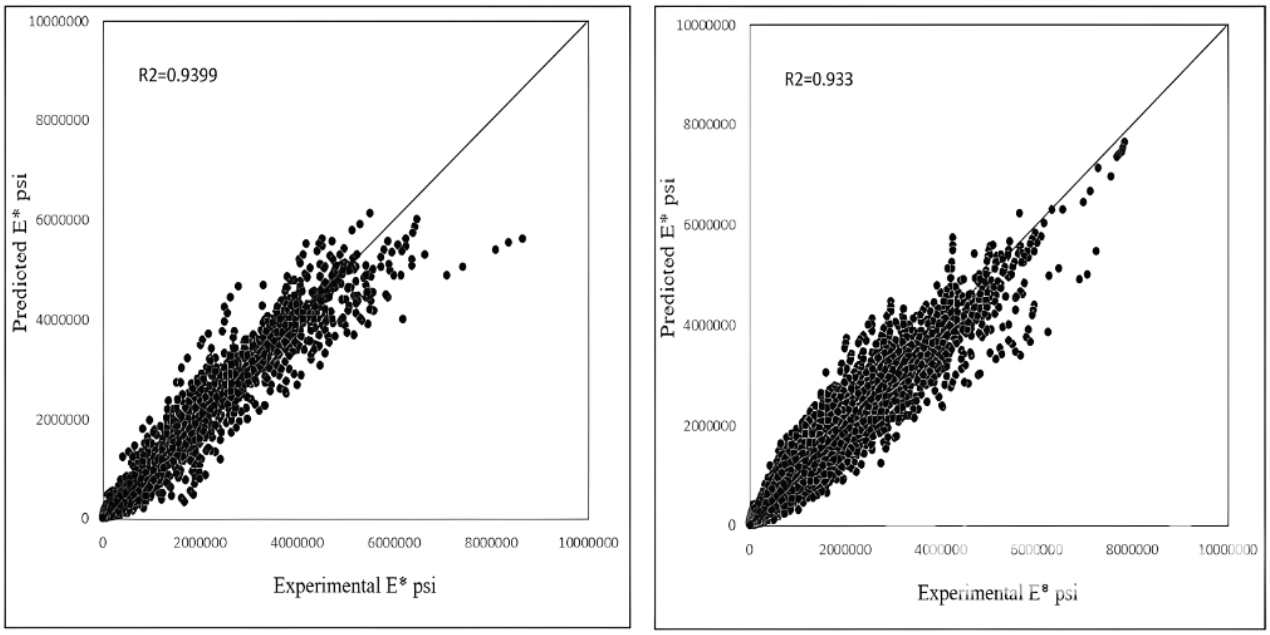

Figure 6. The relationship between experimental E* and anticipated E * in the testing model 1 & 2

ANN can predict E* using experimental data, and by using the equations for bias and weight average for the input data, hidden variables, and output result, it can generate the Equation 1:

$$E^* = \frac{1}{1+e^{-3.60+\frac{-1.62}{1+e^{-A}}+\frac{0.80}{1+e^{-B}}+\frac{0.27}{1+e^{-C}}+\frac{-1.26}{1+e^{-D}}+\frac{1.47}{1+e^{-E}}+\frac{-0.21}{1+e^{-F}}+\frac{-0.14}{1+e^{-G}}+\frac{-0.057}{1+e^{-H}}+\frac{-0.227}{1+e^{-I}}+\frac{-2.72}{1+e^{-J}}+\frac{0.16}{1+e^{-K}}+\frac{-0.45}{1+e^{-L}}}} \quad (1)$$

$A=0.25-0.55*T+0.01*F_C+5.48*|G^*|+0.59*\delta_b+0.24*\rho_{34}-2.06*\rho_{38}-6.1*\rho_4+9.01*\rho_{200}+0.001*AC-0.29*V_a-14.57*V_{beff}+1.31*h$

$B=9.27+0.064*T-0.04*F_C-0.85*|G^*|-0.08*\delta_b-0.0002*\rho_{34}+0.41*\rho_{38}+0.1*\rho_4+3.57*\rho_{200}-0.02*AC+0.028*V_a+2.01*V_{beff}-0.08*h$

$C=19.7+0.082*T+0.06*F_C+1.05*|G^*|+0.17*\delta_b-0.005*\rho_{34}+0.20*\rho_{38}-0.44*\rho_4+24.11*\rho_{200}-0.12*AC-0.07*V_a-2.65*V_{beff}+0.2*h$

$D=-2.5-0.65*T+0.49*F_C-3.48*|G^*|-0.42*\delta_b+0.3*\rho_{34}+0.57*\rho_{38}+1.28*\rho_4+12.02*\rho_{200}+0.14*AC+0.21*V_a+7.12*V_{beff}+0.38*h$

$E=-3.19-0.1*T+5.02*F_C+17.69*|G^*|+0.35*\delta_b-1.08*\rho_{34}+98.93*\rho_{38}-97.76*\rho_4-8.56*\rho_{200}-11.43*AC+0.42*V_a+6.7*V_{beff}-0.49*h$

$F=109.68+0.16*T-0.75*F_C-18.66*|G^*|-3.12*\delta_b+1.16*\rho_{34}-2.26*\rho_{38}+33.53*\rho_4+11.76*\rho_{200}+10.91*AC+1.23*V_a-61.61*V_{beff}+6.01*h$

$G=-58.29+0.05*T+0.18*F_C-55.68*|G^*|-0.16*\delta_b-0.4*\rho_{34}+1.58*\rho_{38}-65.65*\rho_4+30.6*\rho_{200}-10.24*AC-0.19*V_a+35.83*V_{beff}-3.56*h$

$H=-49.43-0.23*T-1.44*F_C-8.89*|G^*|+2.26*\delta_b-0.36*\rho_{34}+19.66*\rho_{38}-94.21*\rho_4+8.12*\rho_{200}+1.49*AC-1.31*V_a-31.96*V_{beff}+0.34*h$

$I=1.72+0.07*T+0.07*F_C-16.55*|G^*|-0.14*\delta_b-0.63*\rho_{34}-16.53*\rho_{38}-1.8*\rho_4-29.17*\rho_{200}+4.94*AC-0.23*V_a-48.34*V_{beff}-0.29*h$

$J=2.11-0.18*T-0.39*F_C-21.05*|G^*|+0.2*\delta_b+0.08*\rho_{34}-21.16*\rho_{38}+196.22*\rho_4-31.76*\rho_{200}-6.12*AC+0.017*V_a-1.52*V_{beff}-4.93*h$

$K=-779.65-0.18*T-3.83*F_C+27.67*|G^*|-1.86*\delta_b+3.13*\rho_{34}+42.97*\rho_{38}+198.21*\rho_4+23.16*\rho_{200}+6.43*AC+0.049*V_a-12.76*V_{beff}+8.39*h$

$L=1.83-0.13*T+5.73*F_C+1.99*|G^*|-0.003*\delta_b-2.9*\rho_{34}-6.01*\rho_{38}-177.11*\rho_4-34.01*\rho_{200}+0.21*AC+37*V_a-721.21*V_{beff}+2.88*h$

The construction of neural model 2, as shown in Figure 7, involves several input parameters on the left side, which correspond to the eight previously mentioned parameters. Model 2 incorporates eight selected input parameters and one hidden layer with two neurons. This simpler architecture achieved R^2 values of 0.932 and 0.933 in training and testing respectively, balancing model simplicity with strong performance. By adjusting the number of hidden layers until the optimal model was created, the number of neurons was set to two. A single neuron on the right side of the brain represents E*. Figure 8 compares the measured E* with observations of the predicted robust E*. The ANN model provides exact values of 0.932 and 0.933 for training and testing, respectively. Figure 8 demonstrates the strong correlation between observed E* and measured E*.

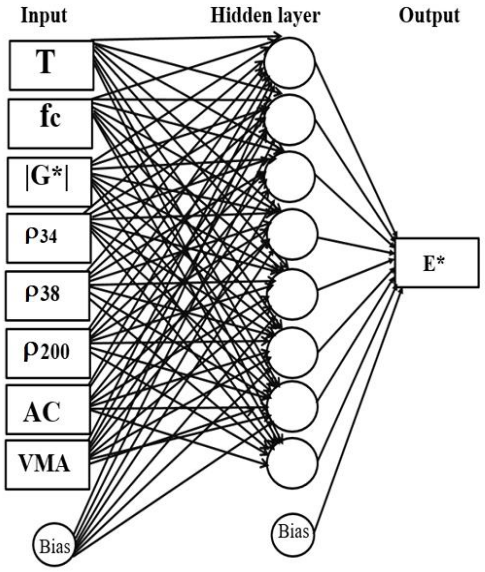

Figure 7. Input parameters, the output of hidden layers, and bias for model 2 are represented by the structure of an ANN

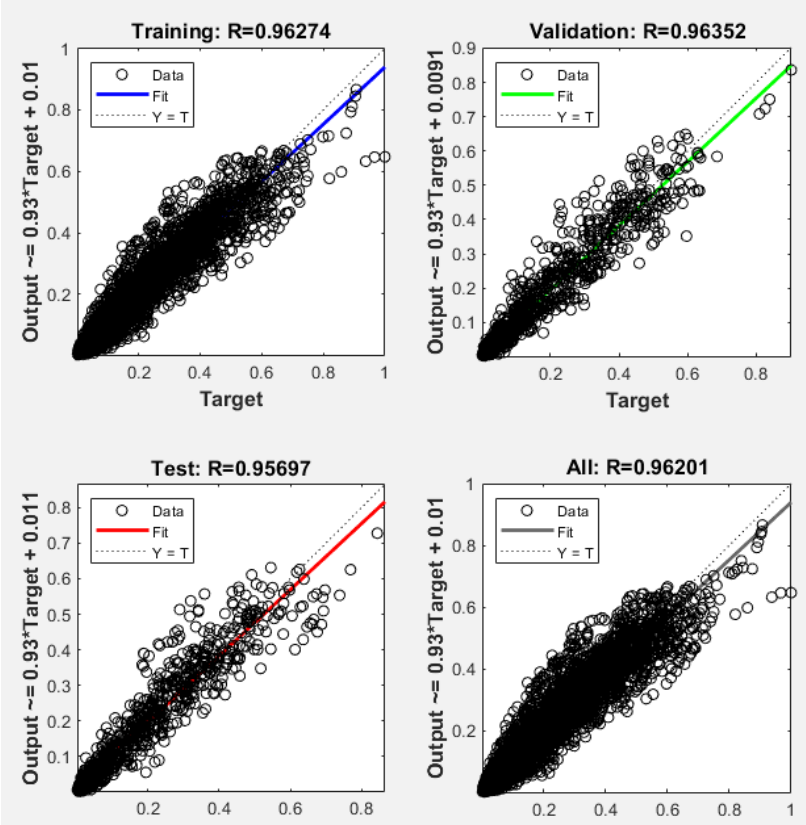

Figure 8. Model 2 training and testing data regression scheme of projected E* against experimental E*

Figure 9 shows the comparison of experimental vs. Predicted E for ANN Model 2*, Model 2 maintains a reliable performance across the validation data. The plot further confirms the model's utility in predicting E* within acceptable error margins. With the use of experimental data, ANN can predict E* and generate Equation 2 by employing the Equations for bias and weight average for input data, hidden results, and output results.

$$E^*=\frac{1}{1+e^{-7.57+\frac{10.84}{1+e^{-A}}+\frac{-6.49}{1+e^{-B}}+\frac{5.32}{1+e^{-C}}+\frac{-10.56}{1+e^{-D}}+\frac{-0.9}{1+e^{-E}}+\frac{0.52}{1+e^{-F}}+\frac{1.06}{1+e^{-G}}+\frac{-3.21}{1+e^{-H}}+\frac{-0.25}{1+e^{-I}}}} \quad (2)$$

A= -10.36+0.068*T-0.048*fc+0.079*|G*|-2.58*ρ_{34}-7.37*ρ_{38}+3.98*ρ_{200}-4.06*AC+4.039*VMA

B= -.655+0.119*T-0.09*fc+0.019*|G*|-0.024*ρ_{34}+0.109*ρ_{38}-.27*ρ_{200}-.069*AC+.527*VMA

C= 2.93-.45*T+0.13*fc+1.22*|G*|+0.16*ρ_{34}+.007*ρ_{38}-0.22*ρ_{200}+.037*AC+.68*VMA

D= -7.56-.069*T-0.049*fc+.074*|G*|+2.10*ρ_{34}-9.63*ρ_{38}+5.27*ρ_{200}-3.88*AC+4.55*VMA

E= -4.55+ 0.80*T-0.008*fc+0.21*|G*|-9.99*ρ_{34}-0.83*ρ_{38}+3.47*ρ_{200}+1.07*AC+1.71 *VMA

F=3.38+ 0.70*T-0.16*fc-0.065*|G*|+3.47*ρ_{34}-10.68*ρ_{38}-1.36*ρ_{200}-3.75*AC-1.46 *VMA

G= -2.71+ 0.35*T+0.059*fc+0.087*|G*|-6.13*ρ_{34}+1.05*ρ_{38}+2.32*ρ_{200}+0.16*AC+1.23*VM

H= 1.098+0.07*T+0.016*fc-0.028*|G*|+0.36*ρ_{34}-1.16*ρ_{38}-0.55*ρ_{200}-0.066*AC-0.13*VMA

I= 0.117 -0.48*T+4.18*fc+0.58*|G*|+.024*ρ_{34}-.016*ρ_{38}-.099*ρ_{200}+0.062*AC+0.0085*VMA

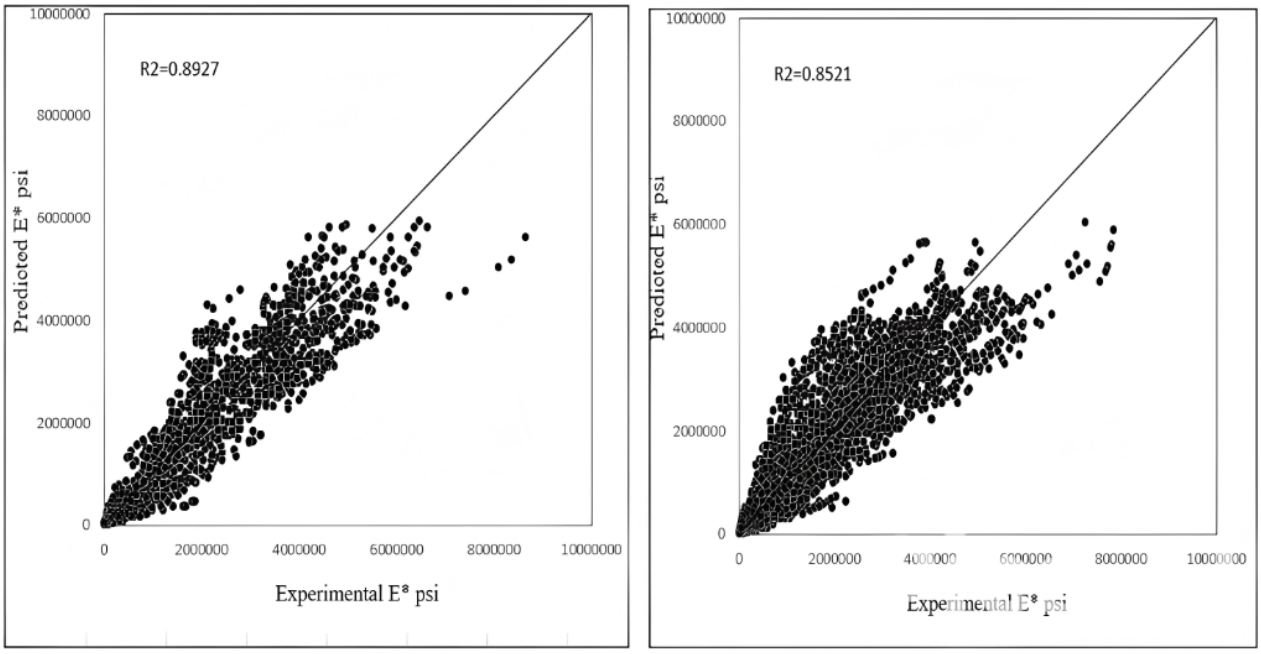

Figure 9. The relationship between experimental E* and predicted E* in training models 1 & 2

After running both models and comparing the R^2 values, it was found that the first model, with an R^2 value of 0.962, outperforms the second one. The first model used twelve neurons and one hidden layer, while the second model used nine neurons and one hidden layer, yielding a value of 0. 931. Table 3 presents the key training parameters used for developing the Artificial Neural Network (ANN) model in this study. The learning rate was set to 0.01 to ensure gradual convergence during the training process, minimizing the risk of overshooting optimal weights. The model was trained for 1000 epochs, allowing sufficient iterations for the weights to adjust and minimize prediction errors. The dataset was divided into 70% for training, 15% for validation, and 15% for testing, ensuring that the model's generalization ability could be objectively assessed. The Levenberg-Marquardt optimization algorithm was selected for its fast convergence properties, especially in regression tasks involving moderate-sized networks. A sigmoid activation function was used to introduce non-linearity into the model, enabling it to learn complex relationships between input variables and the output dynamic modulus (E*). The mean squared error (MSE) was employed as the loss function to quantify prediction accuracy during training [37-39].

Table 3. ANN Training Parameters

Parameter	Value
Learning Rate	0.01
Epochs	1000
Training/Validation/Test Split	70% / 15% / 15%
Optimizer	Levenberg-Marquardt
Activation Function	Sigmoid
Loss Function	MSE (Mean Squared Error)

3.2. Genetic Algorithm Models

The operation of the software is based on chromosomes comprising genes and expression trees that encode genetic information recorded in the chromosome. By creating a link between E* and the temperature of the input, the Gene

Expression Program (GeneXpro5.0) serves as a key tool for saving effort and time in the computation of the dynamic modulus (E*) with temperature (T). Model 1 found a link between E* and eight inputs: temperature (T), frequency (f_c), shear modulus (|G*|), gradation of the mixture (4, 34, 38, and 200), asphalt content (AC), mix air void (V_a percent), effective binder content of the mixture (V_{beff} percent), and viscosity (h) (34, 38, and 200). Model two, on the other hand, focused on asphalt content (AC) and void mineral aggregate (VMA).

The program undergoes multiple iterations, with model 1 set to 50,000 and model 2 set to 100,000 generations, to identify the optimal models. We terminated the experiment and selected the best models based on predefined standards, which included a determination coefficient R^2 greater than 0.7358 for training data and above 0.717087 for testing data in the first model. Similarly, for the second model, R^2 values exceeding 0.6471 and 0.6143 are utilized for testing and training data. Respectively. The Figures 10 and 11 illustrate the results of the predicted E^* against the experimental E^*. The genetic algorithm models provide a decent estimate, with R^2 values of 0.7358 and 0.717087 for training and testing, respectively, as shown in Figures 10 and 11.

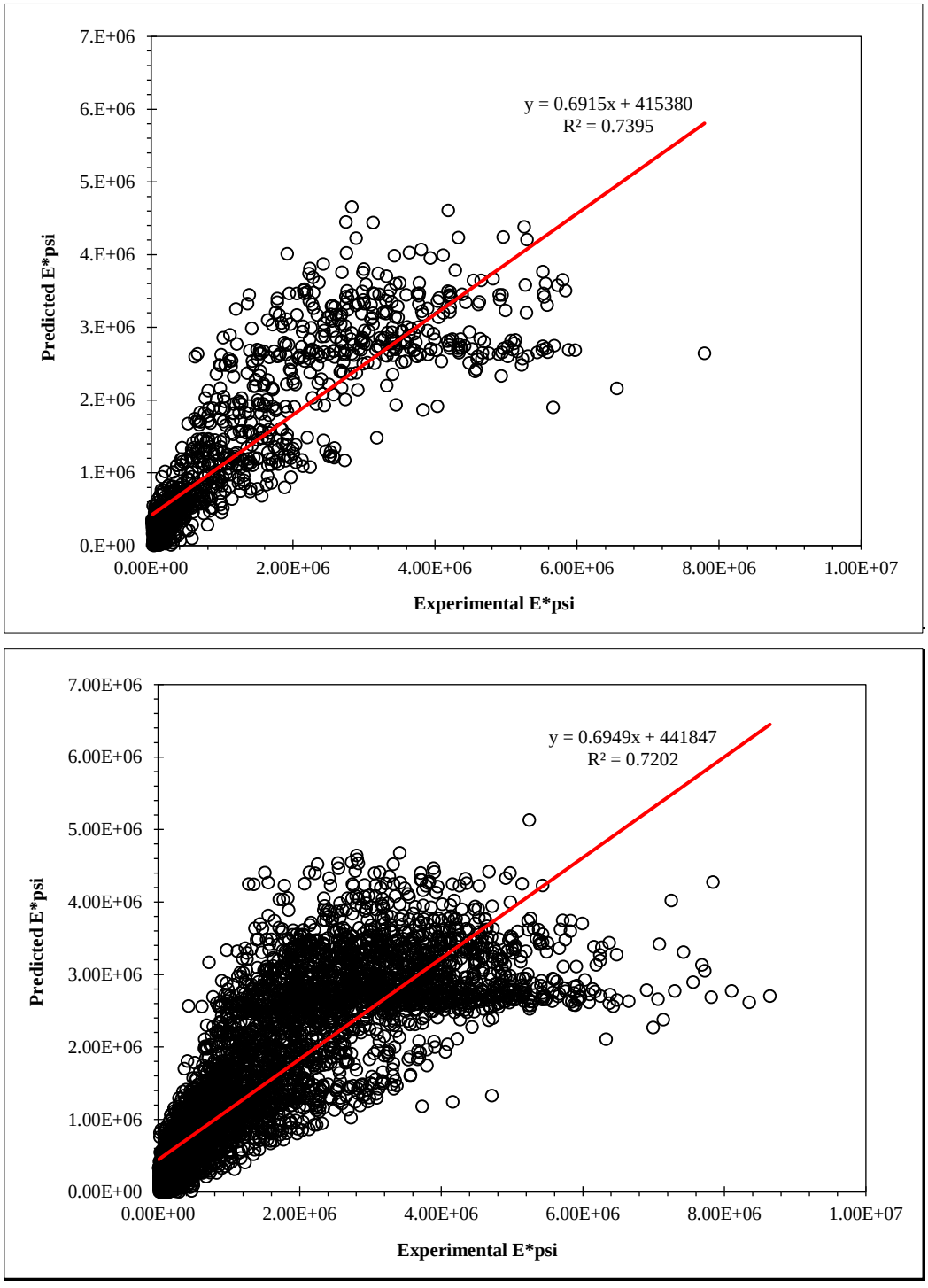

Figure 10. training and testing data of experimental E* against predicted E* regression plot (model 1)

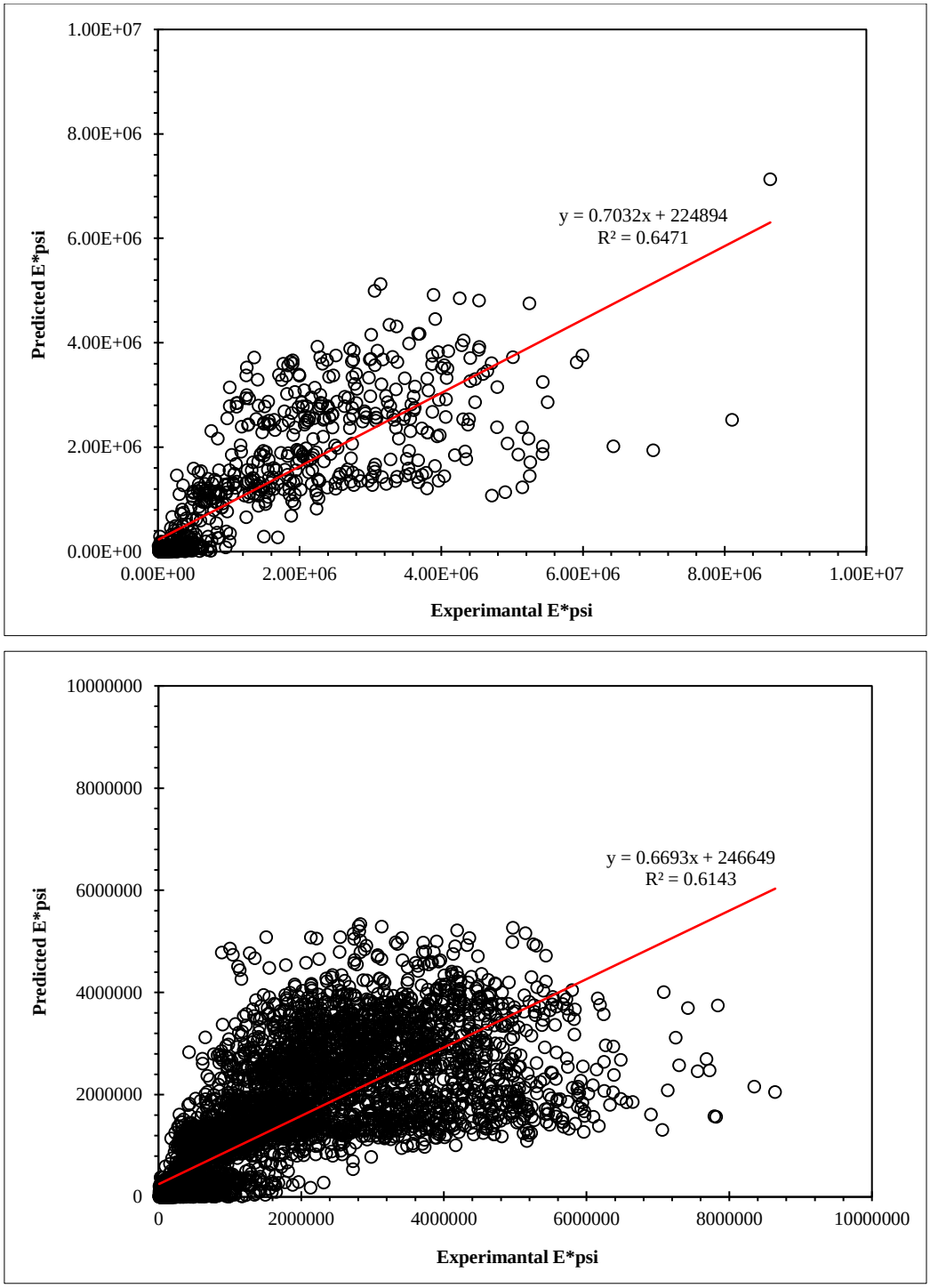

Figure 11. training and testing data of experimental E* against predicted E* regression plot (Model 2)

The Gene Expression Program presents the model as an expression tree and then uses the algorithm system to translate it into a scientific form, as shown in the equations below. In these equations, d defines the inputs, and C is a variable within this program's visual basic language. The sum of the four subtrees is E* (G1, 2, 3, 4). As demonstrated in Figures 12 and 13, the genetic algorithm models are incorporated in the formula derived from expression trees. The empirical equations for (E*) indicate the generation and conversion of four sub-trees (Sub-ET-1, 2, 3, and 4) into an analytical equation form.

E*=G1(Sub-ET-1) +G2(Sub-ET-2) +G3(Sub-ET-3) +G4(Sub-ET-4)

$$E^*=\left(4.81*\left(\left(22.85+\frac{-5.76+\rho_{200}}{2}\right)*\left(\left(|G^*|-db\right)+9.75\right)\right)\right)+\left(\sqrt[3]{h}+\frac{\left(\left((db^*-9.71)*Vbeff\right)-|G^*|\right)}{\tan\frac{1}{db}}\right)+\left(\left(T^*\tan\left(|G^*|+1.16\right)\right)*\left(2|G^*|+db^2\right)\right)+\left(\left(T^*\tan\left(|G^*|+1.16\right)\right)*\left(-9.27-\left(2|G^*|+db^2\right)\right)\right) \quad (3)$$

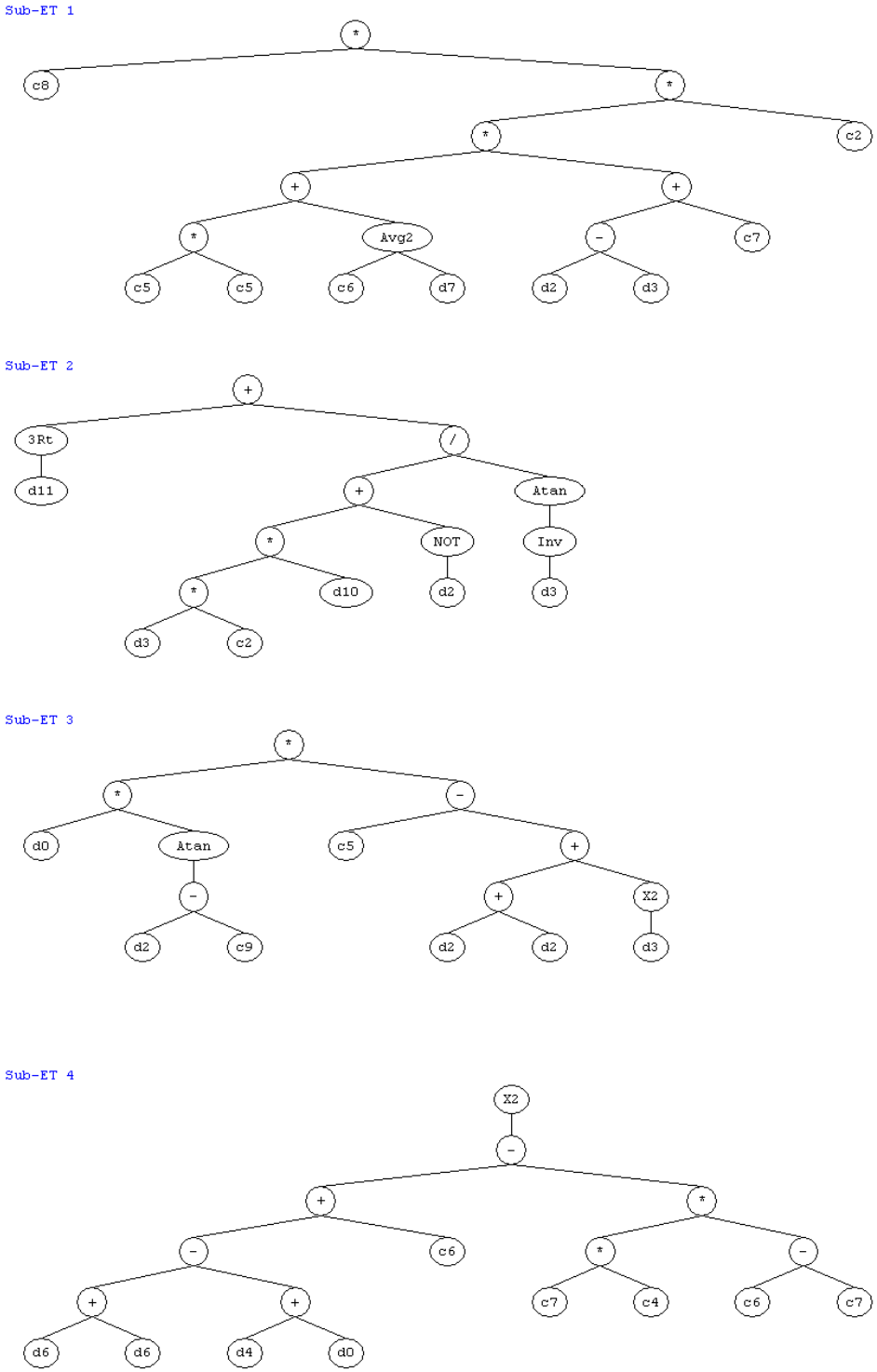

Figure 12. Tree expression to estimate E* from model 1

The strength and effectiveness of the evolutionary neural network and algorithm models were investigated through the R^2 determination coefficients. The R^2 value is found to be a reliable match between predicted and experimental E^* values. The genetic algorithm model provides a reliable assessment, giving an R^2 value of 0.7358 for training, whereas the ANN does a dependable evaluation and offers an R^2 value of 0.95 for training. This suggests that the neural network model outperforms genetic algorithms in predictive accuracy. The novelty of this study depends on the integration of artificial neural networks and genetic algorithms for predicting dynamic modulus, an area not previously examined in the literature. This study introduces two new empirical equations that offer a more precise and computationally successful alternative to existing models, effectively addressing significant drawbacks in current pavement design methodologies. Compared to traditional regression-based models, the proposed ANN and GA models better capture complex nonlinear interactions in the data. This makes them better at predicting E across a range of temperatures and loading frequencies.

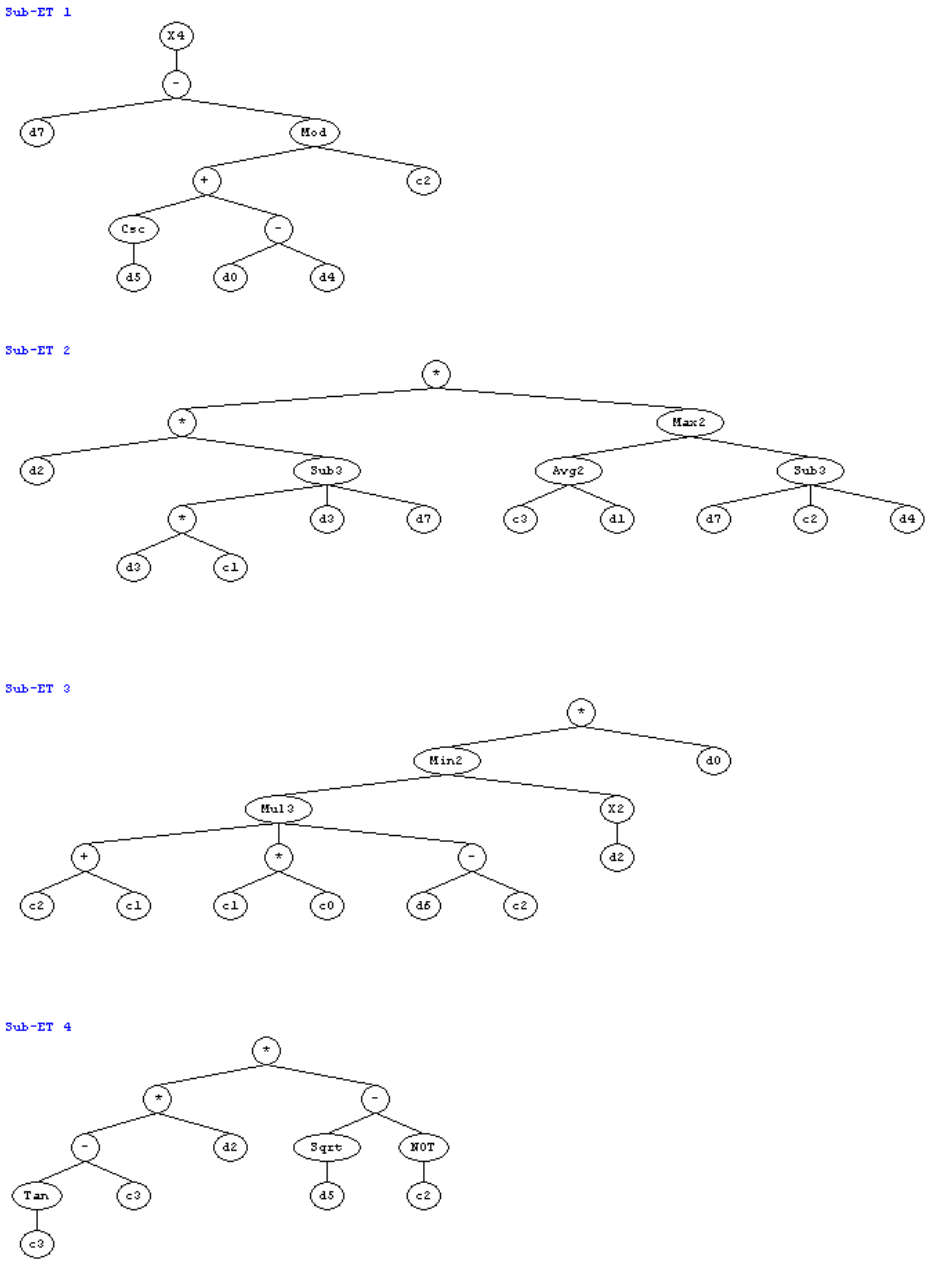

Figure 13. Tree expression to estimate E* from model 2

The empirical equation derived from ANN Model 1 is expressed as:

$$E^*=\left((\text{VMA}-(\text{mod}((\text{Csc}\ \rho_{200}+(\text{T}-\rho_{38})),-14.10))^4\right)+\left(\left(|G^*|^*\left(\left(\rho_{34}*0.84\right),\rho_{34},\ \text{VMA}\right)\right)*\left(\max\left(\frac{1.64+\text{fc}}{2},\left(\text{VMA},-0.72,\rho_{38}\right)\right)\right)\right)+$$
$$\left(\left(\min\left((-4.55-9.99)*(-9.99*9.16)*\left(\sqrt{\rho_{200}}+4.55\right)\right),|G^*|^2\right)*\text{T}\right)+\left((-4.61*|G^*|)*\left(\sqrt{\rho_{200}}+5.11\right)\right) \quad (4)$$

E* = f (T, f_c, |G*|, ρ_{034}, ρ_{038}, ρ_{200}, AC, VMA) with weights and biases detailed in Equation 4.

The GA-derived empirical model (Model 1) is given in functional form as:

E* = G1(SubET1) + G2(SubET2) + G3(SubET3) + G4(SubET4)

where each SubET expression is mathematically derived from the GeneXpro5 tree structure

4. Comparison with Previous Studies

The proposed ANN model performed much better than the Witczak (R^2 = 0.85) and Hirsch (R^2 = 0.80) models, achieving an R^2 value of 0.96. This enhancement becomes particularly significant at high temperatures and low frequencies, when conventional models typically do not perform as well. The GA model is not as precise as the ANN

model, but it is still an acceptable choice, with an R^2 value of 0.73. With a R^2 of 0.96, a mean absolute error (MAE) of 0.05, and a root mean square error (RMSE) of 0.07, the artificial neural network (ANN) model that was made was very accurate. The metrics show that the ANN model exhibits high accuracy and reliability, especially in extreme conditions, including elevated temperatures and low frequencies. With a R^2 of 0.73, a mean absolute error of 0.12, and a root mean square error of 0.15, the proposed Genetic Algorithm (GA) model was not as good as the Witczak models [24] and Hirsch models [9]. The Witczak model worked well at moderate temperatures, with R^2 of 0.85, a mean absolute error of 0.10, and a root mean square error of 0.13. But it became less reliable when temperatures got too high or too low. The Hirsch model exhibited a coefficient of determination of 0.80, a mean absolute error (MAE) of 0.11, and a root mean square error (RMSE) of 0.14. It demonstrated a tendency to miscalculate the modulus of elasticity at elevated temperatures, potentially resulting in conservative predictions for high-temperature applications. The ANN model is the most robust and accurate, particularly in extreme conditions, whereas the GA, Witczak, and Hirsch models are appropriate choices for moderate circumstances. This study includes several limitations; relying on the LTPP database indicates that the models may insufficiently represent the characteristics of asphalt mixtures over the dataset's scope, particularly those with unconventional components or under extreme conditions. The ANN and GA models may not be able to be used in places with limited resources because they require a lot of computing power. In the future, researchers should focus on expanding the dataset to include a wider range of mix types, looking into hybrid modeling approaches, and testing the models with different datasets to see if they can be used in other situations. Table 4 summarizes and contrasts performance metrics of this study's models versus Witczak, Hirsch, ANN-GWO, and ANN-PSO models. The ANN model developed in this study outperforms others in conditions involving high temperatures and low frequencies. This is attributed to the ANN's ability to capture nonlinear interactions that traditional regression models overlook.

Table 4. Comparative Analysis of Model Performance

Model	R^2	MAE	RMSE	Strengths	Weaknesses
ANN (Model 1)	0.96	0.05	0.07	High accuracy in extreme conditions	Requires computational resources
ANN-PSO	0.94	0.06	0.08	Good feature selection and optimization	Sensitive to initial parameters
ANN-GWO	0.93	0.06	0.09	Robust training and tuning	Higher computation time
GA (Model 1)	0.73	0.12	0.15	Acceptable for general predictions	Less reliable in extreme conditions
Witczak	0.85	0.1	0.13	Widely accepted, moderate temperatures	Fails at high/low temperature ranges
Hirsch	0.8	0.11	0.14	Conservative predictions at high temperatures	Tends to underpredict modulus

5. Conclusion

The dynamic modulus, employing the input variables outlined above, was predicted using both ANN and genetic algorithms. The artificial neural network proves to be a reliable technique for E* prediction. The MATLAB software got an R^2 value of 0.96 for training data and 0.95 for testing data in the first model by adding twelve neurons to model 1 and eight neurons to model 2 in the hidden layer, fine-tuning the model for best performance, and getting a high R^2 value. Conversely, the genetic algorithm provided an R^2 value of 0.73 for training data and 0.71 for testing data. The closeness of these numbers to one signifies an acceptable level of precision in the determination coefficient (R^2). In the second model, the MATLAB-derived R^2 values were 0.85 and 0.89 for training and testing data, respectively. The genetic algorithm yielded results of 0.64 and 0.613 for training and testing data, respectively. Summarizing the results of this experiment, the MATLAB-derived R^2 was 0.96, while the genetic algorithm model yielded an R^2 of 0.73. A comparative analysis of the models revealed that MATLAB provided a superior R^2 value. It is concluded that the dynamic modulus is directly proportional to temperature, frequency, and air void ratio. It might be interesting to compare the equation that came out of this study to the MPEDG equation in the future, using different input samples to see how well they work with samples that weren't used in our model.

6. Declarations

6.1. Author Contributions

Conceptualization, S.M.H.; methodology, S.M.H.; software, R.A.A.; validation, F.I.A., S.A., and Z.A.; formal analysis, F.I.A.; investigation, Z.A.; resources, S.A.; data curation, R.A.A.; writing—original draft preparation, S.M.H. and R.A.A.; writing—review and editing, R.A.A.; visualization, F.I.A.; supervision, S.M.H.; project administration, S.M.H.; funding acquisition, S.M.H. All authors have read and agreed to the published version of the manuscript.

6.2. Data Availability Statement

The data presented in this study are available in the article.

6.3. Funding

The authors received no financial support for the research, authorship, and/or publication of this article.

6.4. Conflicts of Interest

The authors declare no conflict of interest.

7. References

[1] NCHRP. (2004). Guide for mechanistic-empirical design of new and rehabilitated pavement structures, national cooperative highway research program. National Cooperative Highway Research Program Transportation Research Board National Research Council, (NCHRP), Washington, D.C., United States.

[2] AASHTO (2008). A Manual of Practice-Interim Edition. American Association of State Highway and Transportation Officials, Washington, D.C., United States.

[3] Ghasemi, P. (2018). Performance evaluation of Coarse-Graded Field Mixtures using Dynamic Modulus Results Gained from Testing in Indirect Tension Mode of Testing. Master Thesis, Iowa State University, Ames, United States.

[4] Birgisson, B., Roque, R., Kim, J., & Pham, L. V. (2004). The use of complex modulus to characterize the performance of asphalt mixtures and pavements in Florida, Final Report, UF Project 4910-4504-784-12, The National Academies of Sciences, Engineering, and Medicine, Keck Center, United States.

[5] Arabali, P., Sakhaeifar, M. S., Freeman, T. J., Wilson, B. T., & Borowiec, J. D. (2017). Decision-Making Guideline for Preservation of Flexible Pavements in General Aviation Airport Management. Journal of Transportation Engineering, Part B: Pavements, 143(2), 4017006. doi:10.1061/jpeodx.0000002.

[6] El-Badawy, S., Abd El-Hakim, R., & Awed, A. (2018). Comparing Artificial Neural Networks with Regression Models for Hot-Mix Asphalt Dynamic Modulus Prediction. Journal of Materials in Civil Engineering, 30(7), 4018128. doi:10.1061/(asce)mt.1943-5533.0002282.

[7] Andrei, D., Mirza, W. and Witczak, M.W. (1999) Development of a Revised Predictive Model for the Dynamic (Complex) Modulus of Asphalt Mixtures. NCHRP Report 1-37A, Washington, D.C., United States.

[8] Bari, J., & Witczak, M. W. (2007). New predictive models for viscosity and complex shear modulus of asphalt binders: for use with mechanistic-empirical pavement design guide. Transportation Research Record, 2001, 9–19. doi:10.3141/2001-02.

[9] Christensen, D. W., Pellinen, T., & Bonaquist, R. F. (2003). Hirsch model for estimating the modulus of asphalt concrete. Asphalt Paving Technology: Association of Asphalt Paving Technologists-Proceedings of the Technical Sessions, 72, 97–121.

[10] Jamrah, A., Kutay, M. E., & Öztürk, H. I. (2014). Characterization of asphalt materials common to Michigan in support of the implementation of the mechanistic-empirical pavement design guide. Transportation Research Record 93rd Annual Meeting Compendium Papers, Kiribati, United States.

[11] Al-Khateeb, G., Shenoy, A., Gibson, N., & Harman, T. (2006). A new simplistic model for dynamic modulus predictions of asphalt paving mixtures. Journal of the Association of Asphalt Paving Technologists, 75.

[12] Sakhaeifar, M. S., Richard Kim, Y., & Garcia Montano, B. E. (2017). Individual temperature based models for nondestructive evaluation of complex moduli in asphalt concrete. Construction and Building Materials, 137, 117–127. doi:10.1016/j.conbuildmat.2016.12.145.

[13] Zhang, C., Ildefonzo, D. G., Shen, S., Wang, L., & Huang, H. (2023). Implementation of ensemble Artificial Neural Network and MEMS wireless sensors for In-Situ asphalt mixture dynamic modulus prediction. Construction and Building Materials, 377, 131118. doi:10.1016/j.conbuildmat.2023.131118.

[14] Huang, J., Zhang, J., Li, X., Qiao, Y., Zhang, R., & Kumar, G. S. (2023). Investigating the effects of ensemble and weight optimization approaches on neural networks' performance to estimate the dynamic modulus of asphalt concrete. Road Materials and Pavement Design, 24(8), 1939–1959. doi:10.1080/14680629.2022.2112061.

[15] Qiao, J., & Wang, L. (2021). Nonlinear system modeling and application based on restricted Boltzmann machine and improved BP neural network. Applied Intelligence, 51(1), 37-50. doi:10.1007/s10489-019-01614-1.

[16] Amaral, H. F., Urrutia, S., & Hvattum, L. M. (2021). Delayed improvement local search. Journal of Heuristics, 27(5), 923-950. doi:10.1007/s10732-021-09479-9.

[17] Zhang, J., Zhang, J., Cao, D., Ding, Y., & Zhou, W. (2023). Mechanistic analysis of bottom-up crack in asphalt pavement using cohesive zone model. Theoretical and Applied Fracture Mechanics, 125, 103904. doi:10.1016/j.tafmec.2023.103904.

[18] Huang, G., Zhang, J., Hui, B., Zhang, H., Guan, Y., Guo, F., Li, Y., He, Y., & Wang, D. (2023). Analysis of Modulus Properties of High-Modulus Asphalt Mixture and Its New Evaluation Index of Rutting Resistance. Sustainability (Switzerland), 15(9), 7574. doi:10.3390/su15097574.

[19] Behnood, A., & Golafshani, E. M. (2021). Predicting the dynamic modulus of asphalt mixture using machine learning techniques: An application of multi biogeography-based programming. Construction and Building Materials, 266, 120983. doi:10.1016/j.conbuildmat.2020.120983.

[20] Acharjee, P. K., Souliman, M. I., Freyle, F., & Fuentes, L. (2024). Development of Dynamic Modulus Prediction Model Using Artificial Neural Networks for Colombian Mixtures. Journal of Transportation Engineering, Part B: Pavements, 150(1), 4023038. doi:10.1061/jpeodx.pveng-1402.

[21] Wang, D., Luo, C., Li, J., & He, J. (2024). Study on Dynamic Modulus Prediction Model of In-Service Asphalt Pavement. Buildings, 14(8), 2550. doi:10.3390/buildings14082550.

[22] Uwanuakwa, I. D., Amir, I. Y., & Umba, L. N. (2024). Enhanced asphalt dynamic modulus prediction: A detailed analysis of artificial hummingbird algorithm-optimised boosted trees. Journal of Road Engineering, 4(2), 224–233. doi:10.1016/j.jreng.2024.05.001.

[23] Hu, S., Zhou, N., Steger, R., Bausano, J., Mahmoud, E., & Zhou, F. (2025). Development of the AI-powered ideal-E* test. Road Materials and Pavement Design, 1–25. doi:10.1080/14680629.2025.2498633.

[24] Zeiada, W., Obaid, L., El-Badawy, S., El-Hakim, R. A., & Awed, A. (2025). Benchmarking Classical and Deep Machine Learning Models for Predicting Hot Mix Asphalt Dynamic Modulus. Civil Engineering Journal (Iran), 11(1), 76–106. doi:10.28991/CEJ-2025-011-01-06.

[25] Witczak, M. W., & Fonseca, O. A. (1996). Revised predictive model for dynamic (complex) modulus of asphalt mixtures. Transportation Research Record, 1540, 15–23. doi:10.3141/1540-03.

[26] Mohammad, L. N., Wu, Z., Obulareddy, S., Cooper, S., & Abadie, C. (2006). Permanent deformation analysis of hot-mix asphalt mixtures with simple performance tests and 2002 mechanistic-empirical pavement design software. Transportation Research Record, 1970, 133–142. doi:10.3141/1970-16.

[27] Georgouli, K., Loizos, A., & Plati, C. (2016). Calibration of dynamic modulus predictive model. Construction and Building Materials, 102, 65–75. doi:10.1016/j.conbuildmat.2015.10.163.

[28] Yousefdoost, S., Vuong, B., Rickards, I., Armstrong, P., & Sullivan, B. (2013). Evaluation of Dynamic Modulus Predictive Models for Typical Australian Asphalt Mixes. 15th AAPA International Flexible Pavements Conference, 19, 1–18.

[29] Wang, H., Al-Qadi, I. L., Faheem, A. F., Bahia, H. U., Yang, S. H., & Reinke, G. H. (2011). Effect of mineral filler characteristics on asphalt mastic and mixture rutting potential. Transportation Research Record, 2208(2208), 33–39. doi:10.3141/2208-05.

[30] Far, M. S. S. (2011). Development of New dynamic modulus (E*) predictive models for Hot Mix asphalt mixtures. Ph.D. Thesis, North Carolina State University, Raleigh, United States.

[31] Ahmad, S., Parvez, M., Khan, T. A., & Khan, O. (2022). A hybrid approach using AHP–TOPSIS methods for ranking of soft computing techniques based on their attributes for prediction of solar radiation. Environmental Challenges, 9, 100634. doi:10.1016/j.envc.2022.100634.

[32] Aneke, F. I., Onyelowe, K. C., & Ebid, A. M. (2024). AI-Based Estimation of Swelling Stress for Soils in South Africa. Transportation Infrastructure Geotechnology, 11(3), 1049–1072. doi:10.1007/s40515-023-00311-4.

[33] Aneke, F. I., Onyelowe, K. C., Ebid, A. M., Nwobia, L. I., & Adu, J. T. (2022). Predictive models of swelling stress—a comparative study between BP- and GRG-ANN. Arabian Journal of Geosciences, 15(17). doi:10.1007/s12517-022-10706-1.

[34] Onyelowe, K. C., Aneke, F. I., Onyia, M. E., Ebid, A. M., & Usungedo, T. (2023). AI (ANN, GP, and EPR)-based predictive models of bulk density, linear-volumetric shrinkage & desiccation cracking of HSDA-treated black cotton soil for sustainable subgrade. Geomechanics and Geoengineering, 18(6), 497–516. doi:10.1080/17486025.2022.2090621.

[35] Hanandeh, S., Ardah, A., & Abu-Farsakh, M. (2020). Using artificial neural network and genetics algorithm to estimate the resilient modulus for stabilized subgrade and propose new empirical formula. Transportation Geotechnics, 24. doi:10.1016/j.trgeo.2020.100358.

[36] Ikechukwu, A. F., & Mostafa, M. M. H. (2022). Swelling Pressure Prediction of Compacted Unsaturated Expansive Soils. International Journal of Engineering Research in Africa, 59, 119–134. doi:10.4028/p-eq1419.

[37] Kennedy, E. H. (2024). Semiparametric Doubly Robust Targeted Double Machine Learning: A Review. Handbook of Statistical Methods for Precision Medicine, 207–236. doi:10.1201/9781003216223-10.

[38] Onyelowe, K. C., Kontoni, D. P. N., Ebid, A. M., Dabbaghi, F., Soleymani, A., Jahangir, H., & Nehdi, M. L. (2022). Multi-Objective Optimization of Sustainable Concrete Containing Fly Ash Based on Environmental and Mechanical Considerations. Buildings, 12(7), 948. doi:10.3390/buildings12070948.

[39] Onyelowe, K. C., Mojtahedi, F. F., Azizi, S., Mahdi, H. A., Sujatha, E. R., Ebid, A. M., Darzi, A. G., & Aneke, F. I. (2022). Innovative Overview of SWRC Application in Modeling Geotechnical Engineering Problems. Designs, 6(5), 69. doi:10.3390/designs6050069.